Journal of Alloys and Compounds, 184 (1992) 235–242
JALCOM 185

Orbital magnetization and iron contribution to the magnetic anisotropy of $Er_2Fe_{17}C_x$

R. J. Zhou, Cz. Kapusta* and M. Rosenberg
Experimentalphysik VI, Ruhr-Universität Bochum, PB 102148, Bochum (FRG)

K. H. J. Buschow
Philips Research Laboratories, NL-5600 JA Eindhoven (Netherlands)

(Received November 11, 1991)

Abstract

A detailed ^{57}Fe Mössbauer spectroscopy study of the spin reorientation phenomenon in the $Er_2Fe_{17}C_x$ series is presented. From the step-like increase of the effective magnetic field at the spin reorientation temperature the sign and magnitude of the anisotropy of the orbital contribution to the iron hyperfine field are estimated. The spin–orbit contribution to the anisotropy energy is compared with the value of the macroscopic magnetocrystalline anisotropy.

1. Introduction

It was recently found that incorporation of carbon into rare earth (RE) intermetallic compounds of the type RE_2Fe_{17} can significantly increase the crystal-field-induced anisotropy of the RE sublattice. The planar anisotropy of most RE_2Fe_{17} compounds is primarily due to the anisotropy of the iron sublattice. However, for REs with a positive second-order Stevens factor α_J (*e.g.* RE ≡ Sm, Er, Tm), carbon-induced enhancement of the RE anisotropy can lead to a change in the easy magnetization direction (EMD) from the basal plane to the *c* axis. Because of the much stronger temperature dependence of the RE anisotropy, a reorientation of the EMD with temperature may occur. For instance, $Er_2Fe_{17}C_{1.5}$ possesses a uniaxial anisotropy with the EMD parallel to the *c* axis at 4.2 K but reorientation of the EMD to the basal plane takes place in a narrow range around 122–127 K [1]. The carbon concentration dependence of the spin reorientation temperature (T_{sr}) of $Er_2Fe_{17}C_x$ determined by a.c. initial susceptibility measurements was reported by Kou *et al.* [2]. In order to better understand how the local magnetic moments at different iron sites change during the spin reorientation and to estimate the iron contribution to the magnetocrystalline anisotropy, we performed a more detailed Mössbauer effect study on this system in the concentration range $0 \leqslant x \leqslant 1.5$.

*Alexander von Humboldt fellow on leave from Department of Solid State Physics, University of Mining and Metallurgy, 30-059 Cracow, Poland.

2. Experimental details

The sample preparation has already been described elsewhere [2]. X-ray examination showed that the crystallographic structure of $Er_2Fe_{17}C_x$ changes from hexagonal Th_2Ni_{17} type to rhombohedral Th_2Zn_{17} type with increasing carbon concentration. Samples with $x<0.8$ have the hexagonal structure whereas for $x=1.5$ the majority phase is rhombohedral [3]. For some samples with high carbon concentration a small amount of α-Fe was also found.

The ^{57}Fe Mössbauer spectra were taken with a standard set-up equipped with a ^{57}Co(Rh) source at temperatures between 4.2 K and room temperature. The spectra were fitted with a least-squares programme.

3. Results and discussion

The structures of the hexagonal Th_2Ni_{17} type and rhombohedral Th_2Zn_{17}-type phases are closely related. Both structure types comprise four crystallographically non-equivalent iron sites $4f$ ($6c$), $6g$ ($9d$), $12j$ ($18f$) and 12 k ($18h$), where the symbols in parentheses refer to the rhombohedral structure. From symmetry considerations it follows that when the magnetization lies in the basal plane, the Mössbauer spectra have to be fitted by means of six subspectra with relative intensities 4_f:6_g:8_j:8_k:4_j:4_k for the Th_2Ni_{17} type or 6_c:9_d:12_f:12_h:6_f:6_h for the Th_2Zn_{17} type [4]. In the case of uniaxial magnetic anisotropy the Mössbauer spectra can be fitted with four subspectra. A further splitting of the subspectra arising from the influence of carbon neighbours on the j (f) and k (h) sites should be taken into account in the case of carbides. Because of the complex structure of the Mössbauer spectra and the presence of two crystal forms in some samples, only the hyperfine field at the iron dumb-bell site ($4f$ or $6c$) is clearly distinguishable from the contribution of the other sites to the Mössbauer spectra. For this reason we confine our discussion mainly to the average hyperfine field and the hyperfine field at the dumb-bell site as was done previously in ref. 1.

The ^{57}Fe Mössbauer spectra of $Er_2Fe_{17}C_x$ measured at 4.2 K are presented in Fig. 1. One can easily see that the shape of the spectra for samples with $\leqslant 0.5$ is different from that for $x \geqslant 0.8$. The average effective magnetic field ($\overline{B_e}$) and the effective magnetic field at the iron dumb-bell site ($B_e^{f,c}$) derived from the fits are listed in Table 1. The initial increase and following slight decrease in $\overline{B_e}$ with increasing carbon concentration are the result of competition between magnetovolume effects which enhance the iron moment and bonding effects (hybridization of the 3d electrons of iron with the 2p valence electrons of carbon) which may decrease the iron moment as found for $Y_2Fe_{17}C_x$ [1]. The observed increase in $\overline{B_e}$ and especially in $B_e^{f,c}$ with x, however, is much stronger than that observed for the $Y_2Fe_{17}C_x$ compounds. Following the same treatment as used in our previous paper [1], we attribute this additional increase to carbon-induced reorientation of the EMD from the basal plane for $x \leqslant 0.5$ to the c-axis for $x \geqslant 0.8$.

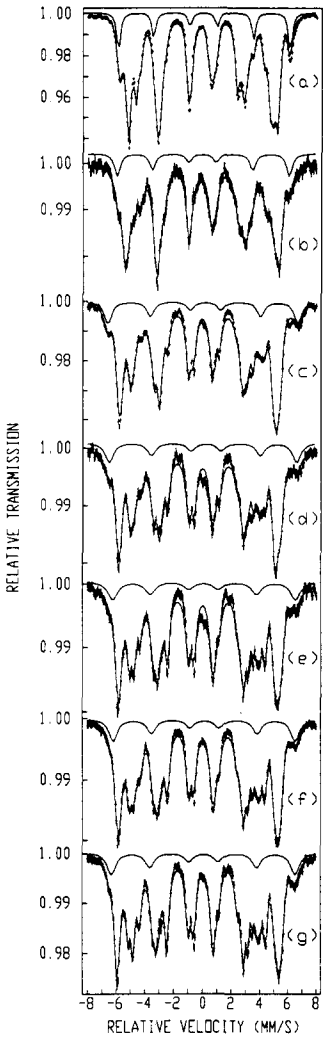

Fig. 1. ^{57}Fe Mössbauer spectra of $Er_2Fe_{17}C_x$ for $x=$ (a) 0.0, (b) 0.5, (c) 0.8, (d) 1.0, (e) 1.2, (f) 1.4 and (g) 1.5 at 4.2 K; ——, subspectrum contributed by the iron dumb-bell site.

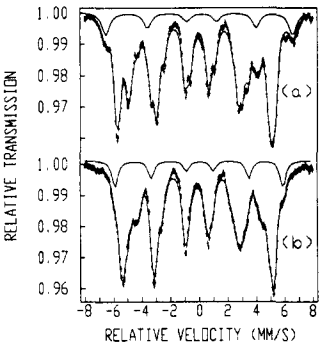

Fig. 2. ^{57}Fe Mössbauer spectra of $Er_2Fe_{17}C_{0.8}$ at (a) 60 and (b) 77 K; ——, subspectrum contributed by the iron dumb-bell site.

In order to determine the spin reorientation temperature and the change in hyperfine field caused by spin reorientation, the Mössbauer spectra of the $Er_2Fe_{17}C_x$ samples with $x=0.8$ have been measured at temperatures between 4.2 K and room temperature. Representative Mössbauer spectra of $Er_2Fe_{17}C_{0.8}$ below and above the spin reorientation temperature are shown in Fig. 2. There is an obvious change in the shape of the spectra owing to the spin reorientation. The temperature dependence of $\overline{B_e}$ and $B_e^{f,c}$ for $Er_2Fe_{17}C_{0.8}$ is

TABLE 1

$\overline{B_e}$ and $B_e^{f,c}$ values of $Er_2Fe_{17}C_x$ derived from Mössbauer spectra taken at 4.2 K and the spin reorientation temperature T_{sr}

x	$\overline{B_e}$ (T)	$B_e^{f,c}$ (T)	T_{sr} (K)
0.0	31.6	37.4	
0.5	32.3	37.5	
0.8	33.0	41.4	76
1.0	32.9	40.9	97
1.2	32.7	40.9	117
1.4	32.4	39.7	120
1.5	32.6	40.0	123

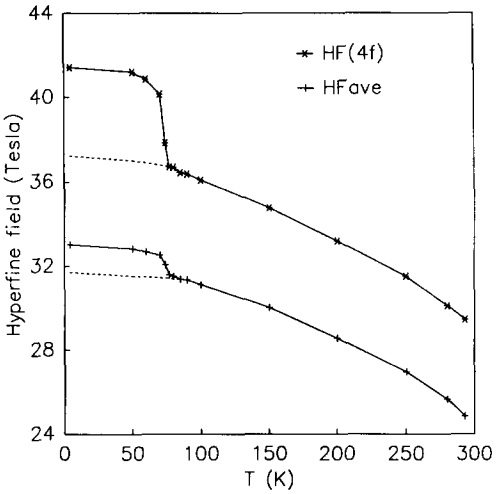

Fig. 3. Temperature dependence of $\overline{B_e}$ and B_e^f of $Er_2Fe_{17}C_{0.8}$.

shown in Fig. 3. One can see that the spin reorientation takes place in a narrow temperature range. From the fits of the spectra we derived the values of the increases in $\overline{B_e}$ (about 1.3 T) and B_e^f (about 4.2 T) which arise as a consequence of the spin reorientation. These values are close to those found for Tm_2Fe_{17} [4]. The spin reorientation temperatures of $Er_2Fe_{17}C_x$ determined from the Mössbauer data are collected in Table 1. The results are in agreement with those of a.c. initial susceptibility measurements reported by Kou *et al.* [2]. Comparing our results with those reported for $Er_2Fe_{17}N_x$ [5], one can see that the spin reorientation temperature range of the Er_2Fe_{17} carbides is narrower than that of the corresponding nitrides. The effective magnetic field at the iron nuclei ($\boldsymbol{B}_e$) can be expressed as

$$\boldsymbol{B}_e = \boldsymbol{B}_{loc} + \boldsymbol{B}_{hf} \quad (1)$$

where $\boldsymbol{B}_{loc}$ is the local field and $\boldsymbol{B}_{hf}$ is the hyperfine field. The local contribution is represented by

$$\boldsymbol{B}_{\mathrm{loc}} = \boldsymbol{B}_{\mathrm{L}} + \boldsymbol{B}_{\mathrm{dip}} \tag{2}$$

where $B_{\mathrm{L}} = \mu_0 M_{\mathrm{s}}/3$ is the Lorentz field and $\boldsymbol{B}_{\mathrm{dip}}$ is the dipolar field

$$\boldsymbol{B}_{\mathrm{dip}} = -\mu_0 \sum \left(\frac{\boldsymbol{\mu}_i}{r_i^3} - \frac{3(\boldsymbol{\mu}_i \cdot \boldsymbol{r}_i)\boldsymbol{r}_i}{r_i^5} \right) \tag{3}$$

The hyperfine contribution can be expressed as

$$\boldsymbol{B}_{\mathrm{hf}} = \boldsymbol{B}_{\mathrm{s}} + \boldsymbol{B}_{\mathrm{orb}} + \boldsymbol{B}_{\mathrm{N}} \tag{4}$$

where the term B_{s} originates from the core and conduction electron polarization by the iron spin moment itself. It is proportional and antiparallel to the iron spin moment μ_{s}. B_{N} is the polarization contribution of the magnetic neighbours via conduction electrons. The contributions B_{s} and B_{N} are isotropic. B_{orb} is the orbital contribution arising from the orbital current of the 3d electrons. It is proportional to the orbital moment μ_{L} and thus anisotropic.

In order to explain the observed change in B_{e} with reorientation of the EMD, possible changes in the two contributions B_{loc} and B_{hf} to B_{e} have been considered. The difference in B_{loc} related to the alignment of the magnetization in the basal plane or along the c axis arises mainly from the anisotropy of the dipolar term B_{dip}, whereas the difference in B_{hf} associated with the two directions is mainly due to B_{orb}. Thus the variations in B_{e} observed upon reorientation of the EMD can be assigned to the difference in the values of B_{dip} and B_{orb} for the magnetic moment alignment in the basal plane ($\perp$) and along the c axis ($\parallel$), *i.e.*

$$\Delta B_{\mathrm{e}} = \Delta B_{\mathrm{dip}} + \Delta B_{\mathrm{orb}} \tag{5}$$

where $\Delta B_{\mathrm{e}} = (B_{\mathrm{e}})_{\perp} - (B_{\mathrm{e}})_{\parallel}$, $\Delta B_{\mathrm{dip}} = (B_{\mathrm{dip}})_{\perp} - (B_{\mathrm{dip}})_{\parallel}$ and $\Delta B_{\mathrm{orb}} = (B_{\mathrm{orb}})_{\perp} - (B_{\mathrm{orb}})_{\parallel}$.

The values of B_{dip} at each iron site in the underlying crystal structure have been computed for the two above-mentioned directions of magnetization using $\mu_{\mathrm{Fe}} = 2\mu_{\mathrm{B}}$, $\mu_{\mathrm{Er}} = -9\mu_{\mathrm{B}}$ and $\mu_{\mathrm{C}} = 0$. All magnetic moments present in a sphere of radius 8.6 Å have been taken into account. For the EMD along the c-axis each of the iron sites is characterized by a single value of B_{dip}. For an arbitrary direction within the basal plane up to three values of B_{dip} at each of the $6g$, $12j$ and $12k$ sites may have to be considered, whereas a single value of B_{dip} at the $4f$ site is appropriate. A similar influence of the orbital contribution on the number of subspectra can be expected. However, as mentioned previously, because of the large uncertainty in both assignment and values of the hyperfine parameters to be associated with the different iron sites, we have restricted ourselves to the analysis of the average values of B_{e} and to the analysis of the B_{e} value belonging to the relatively well-resolved subspectrum of the $4f$ site.

In order to obtain a representative value for $\overline{B_{\mathrm{dip}}}$, we have averaged the values of B_{dip} over all the iron sites. This value together with that of B_{dip} at the $4f$ site (B_{dip}^{f}) are collected in Table 2. Their differences between the basal plane and c-axis directions are included as well. The $\overline{B_{\mathrm{e}}}$ and B_{e}^{f} values of $Er_2Fe_{17}C_{0.8}$ before and after spin reorientation are also listed in Table 2.

TABLE 2

$\overline{B_e}$, B_e^f, $\overline{B_{dip}}$ and B_{dip}^f values of $Er_2Fe_{17}C_{0.8}$ for the magnetic moments in the basal plane ($\perp$) and along the c axis ($\parallel$). The differences between the two directions are also included. A positive sign means the direction of the field is parallel to the iron spin moments

Direction	$\overline{B_e}$ (T)	B_e^f (T)	$\overline{B_{dip}}$ (T)	B_{dip}^f (T)
$\perp$	−31.7[a]	−37.2[a]	−0.07	+0.31
$\parallel$	−33.0	−41.4	+0.13	−0.62
$\perp - \parallel$	+1.3	+4.2	−0.20	+0.93

[a]Extrapolated to 4.2 K.

Taking the values from Table 2 and using eqn. (5), one gets the changes in orbital fields $\overline{\Delta H_{orb}} = (\overline{H_{orb}})_\perp - (\overline{H_{orb}})_\parallel = 1.5$ T and $\Delta H_{orb}^f = (H_{orb}^f)_\perp - (H_{orb}^f)_\parallel = 3.3$ T.

The value of B_{orb} at the ith site of iron is related to the orbital component of the iron magnetic moment μ_L^i:

$$B_{orb}^i = A_L \mu_L^i \tag{6}$$

The value of μ_L depends on the local symmetry of the sites and the orientations of their magnetic moments following changes in the effective orbital momentum L of the d electrons participating in the formation of the local iron magnetic moment. A_L is the orbital hyperfine-coupling constant.

It has been postulated by Streever that the magnetocrystalline anisotropy of the cobalt sublattice in cobalt-containing permanent magnetic materials originates mostly from the spin–orbit interaction [6]. The results obtained by ^{59}Co nuclear magnetic resonance experiments on YCo_5 [6] and $(Nd_x Fe_{1-x})_2Co_{14}B$ [7] allowed the attribution of almost the entire anisotropy energy of the cobalt sublattice to the anisotropy caused by the spin–orbit interaction.

Recent band structure calculations for YCo_5 by means of the FLAPW [8] and LMTO-ASA [9] methods including orbital polarization have shown that there is indeed a strong correlation between the anisotropy energy of the spin–orbit interaction and the change in orbital moment. A quantitative agreement of ΔE with the bulk magnetocrystalline anisotropy was obtained. However, full-potential calculations are limited to small unit cells and cannot be used effectively at present for Re_2Fe_{17} compounds.

Comparing the experimental and theoretical values for the orbital moments in elemental h.c.p. cobalt and b.c.c. iron [10, 11], one can see that the corresponding values for iron ($\mu_L = 0.06 - 0.08$ μ_B) are smaller than those for cobalt ($\mu_L = 0.14$ μ_B). However, in f.c.c. iron the corresponding value is even larger than that in f.c.c. cobalt (0.14 and 0.12 μ_B respectively). Hence one may expect an anisotropy of the spin–orbit interaction in the iron-based compounds. Therefore we tried to estimate the anisotropy of the spin–orbit interaction of iron in the Re_2Fe_{17}-type compounds using the values of ΔB_{orb} obtained in our Mössbauer study.

From the spin–orbit interaction expressed as

$$E_{so} = \lambda \boldsymbol{L} \cdot \boldsymbol{S} \tag{7}$$

one may estimate the contribution to the local anisotropy energies (E_a^i) of the iron sites by means of the expression

$$E_a^i = \frac{1}{2} \lambda \frac{\Delta \mu_L^i}{\mu_B} \frac{\mu_S^i}{\mu_B} \tag{8}$$

where $\Delta \mu_L^i = (\mu_L^i)_\perp - (\mu_L^i)_\parallel$. Using eqn. (2), one obtains

$$E_a^i = \frac{1}{2} \lambda \frac{\Delta B_{orb}^i}{A_L \mu_B} \frac{\mu_S^i}{\mu_B} \tag{9}$$

where $\Delta B_{orb}^i = (B_{orb}^i)_\perp - (B_{orb}^i)_\parallel$.

Using the values $\lambda = -112$ cm^{-1} calculated for the Fe atom [12], $A_L = 42$ T μ_B^{-1} obtained for α-Fe [13] and taking $\mu_S = 2$ μ_B equal for all sites, one finds $E_a^{4f} = -174 \times 10^{-24}$ J atom^{-1} and $\overline{E_a} = -79 \times 10^{-24}$ J atom^{-1}. The negative values of both anisotropy energies mean that the EMD is perpendicular to the c-axis for the iron $4f$ site moments. Since the orbital contribution of the other iron site moments is comparatively weak or absent, this means that the same EMD is adopted by the whole iron sublattice. The value $E_a = K_1 + K_2 = -392$ J kg^{-1} [14] obtained in bulk anisotropy measurements for Y_2Fe_{17} corresponds to -43×10^{-24} J atom^{-1}. Taking this value as representing the iron sublattice anisotropy in the RE_2Fe_{17} series, one can see that the value obtained by us is twice as large. The contribution to the iron anisotropy energy estimated for dipolar interactions is one order of magnitude smaller, so that one cannot assign the discrepancy to this effect. However, the approximations made in our evaluation have introduced a large uncertainty and our result can be treated as a rough estimate only. Nevertheless, it is an indirect confirmation of the preference of the iron moments for planar anisotropy in this compound. The anisotropy of B_{orb} that we found for $Er_2Fe_{17}C_x$ is close to those reported for other RE_2Fe_{17} compounds as well as for their carbides and nitrides [5, 15].

4. Conclusions

Carbon-induced reorientation of the EMD from the basal plane to the c axis is evidenced by a step-like increase in B_e at the iron nuclei. The spin reorientation effects occur in a narrow temperature range of about 10 K. The initial increase in B_e measured at 4.2 K between $x = 0$ and 0.5 and the slight decrease for $x > 1$ are similar to those observed for the yttrium-based series [1] and are attributed to the opposite influences of the magnetovolume and chemical bonding effects. The step-like change in B_e can be assigned mainly to the iron hyperfine field anisotropy in these compounds. The iron spin–orbit contribution to the anisotropy energy estimated on the basis of the change in B_{orb} is of the same order of magnitude as the bulk anisotropy

constant of the iron sublattice in Y_2Fe_{17} and has the correct sign. This statement can be generalized by saying that the magnetocrystalline anisotropy of the iron sublattice in $RE_2Fe_{17}C_x$ and $R_2Fe_{17}N_x$ permanent magnetic materials can be understood in terms of spin–orbit interactions associated with the small orbital contribution to the iron moments in these materials.

Acknowledgments

We kindly acknowledge the support of the Commission of the European Community for organizing scientific meetings and promoting informational cooperation relevant to our research as participants in the programme of the Concerted European Action on Magnets. The financial support of the Alexander von Humboldt foundation for one of us (Cz.K.) is gratefully acknowledged.

References

1 R. J. Zhou, Th. Sinnemann, M. Rosenberg and K. H. J. Buschow, *J. Less-Common Met., 171* (1991) 263.
2 X. C. Kou, R. Grössinger, T. H. Jacobs and K. H. J. Buschow, *Physica B. 168*, (1991) 181–186.
3 M. Gerndorf, *Diplom Thesis*, Ruhr-Universität Bochum, 1992.
4 P. C. M. Gubbens and K. H. J. Buschow, *Phys. Status Solidi A, 4* (1976) 729–735.
5 P. C. M. Gubbens, A. A. Moolenaar, G. J. Boender, A. M. van der Kraan, T. H. Jacobs and K. H. J. Buschow, *J. Magn. Magn. Mater., 97* (1991) 69.
6 R. L. Streever, *Phys. Rev. B, 19* (1979) 2704.
7 Cz. Kapusta and H. Figiel, *J. Phys. (Paris), 49 Colloq. C8*, (1988) 559.
8 R. Coehoorn and G. H. O. Daalderop, *J. Magn. Magn. Mater., 104* (1992) 1081.
9 L. Nordström, M. S. S. Brooks and B. Johansson, *J. Magn. Magn. Mater., 104* (1992) 1942.
10 M. B. Stearns, in *Landoldt–Börnstein, New Series III/19a*, Springer, Berlin, (1986) 24.
11 O. Eriksson, B. Johansson, R. C. Albers, A. M. Boning and M. S. S. Brooks, *Phys. Rev. B, 42* (1990) 2707.
12 S. Fraga, J. Karwowski and K. M. S. Saxena, *At. Data Nucl. Data Tables, 12* (1973) 467.
13 R. Coehoorn, C. J. M. Denissen and R. Eppenga, *J. Appl. Phys., 69* (1991) 6222.
14 B. Matthaei, J. J. M. Franse, S. Sinnema and R. J. Radwanski, *J. Phys. (Paris), 49 Colloq. C8* (1988) 559.
15 P. C. M. Gubbens, A. M. van der Kraan, T. H. Jacobs and K. H. J. Buschow, *J. Magn. Magn. Mater., 80* (1989) 265.